SFB/CPP-05-41
TTP/05-14
hep-ph/0509048
September 2005

Two-loop matching coefficients for the strong coupling in the MSSM

R. Harlander, L. Mihaila, M. Steinhauser

Institut für Theoretische Teilchenphysik, Universität Karlsruhe,

76128 Karlsruhe, Germany

Abstract

When relating the strong coupling α_s, measured at the scale of the Z boson mass, to its numerical value at some higher energy, for example the scale of Grand Unification, it is important to include higher order corrections both in the running of α_s and the decoupling of the heavy particles. We compute the two-loop matching coefficients for α_s within the Minimal Supersymmetric Standard Model (MSSM) which are necessary for a consistent three-loop evolution of the strong coupling constant. Different scenarios for the hierarchy of the supersymmetric scales are considered and the numerical effects are discussed. We find that the three-loop effects can be as large as and sometimes even larger than the uncertainty induced by the current experimental accuracy of $\alpha_s(M_Z)$.

PACS: 12.10.Kt, 12.38.-t, 12.38.Bx, 12.60.Jv

1 Introduction

In spite of describing all current experimental precision data extremely well, it is commonly believed that the Standard Model (SM) is not the ultimate theory of particle physics. This is due to deficiencies like the so-called fine tuning problem which arises from quadratic divergences combined with the large difference between the electro-weak and the Planck scale.

A popular extension of the SM that cures this problem is the so-called Minimal Supersymmetric Standard Model (MSSM). In addition, one of its most attractive features is the possibility of unification of the strong, the weak, and the electro-magnetic coupling constants. While having very different numerical values at the electro-weak scale, they may have a common intersection point at a scale $\mu_{\rm GUT} \sim 10^{16}$ GeV [1–6] which is therefore considered to be the typical scale of a Grand Unified Theory (GUT). In the minimal SM, such an intersection can not be achieved.

The relation of the coupling constants at different energy scales is governed by the renormalization group running, accompanied by the appropriate decoupling of heavy particles, to be described in more detail in Section 2. The most recent studies of the coupling constants at the GUT scale as evolved from their experimental values at the weak scale have been performed in the context of the SUSY Parameter Analysis project (SPA) [8]. It is the purpose of this paper to determine the precise evolution of the strong coupling α_s. In particular, we evaluate the two-loop decoupling relations within the MSSM. In combination with the known beta function, this allows us to determine $\alpha_s(\mu_{\rm GUT})$ at three-loop accuracy, and to estimate its theoretical uncertainty.

The outline of this paper is as follows: in Sections 2 and 3 we review the theoretical framework and introduce our notation. In Section 4 we quote the renormalization constants and the β function in the $\overline{\rm DR}$ scheme within the MSSM. Our results for the decoupling relations are given in Section 5, and the phenomenological implications are discussed in Section 6. Our findings are summarized in Section 7.

2 Decoupling of heavy particles

In the framework of QCD and its supersymmetric extension, it is convenient to use a mass-independent renormalization scheme such as $\overline{\rm MS}$ or $\overline{\rm DR}$. Thus, by construction, the beta function governing the running of α_s is independent of the particle masses. It only depends on the particle content of the underlying theory, i.e., the number of active quarks, squarks and gluinos, denoted by n_f, n_s, and $n_{\tilde{g}}$ in what follows (a more precise definition of these labels is given subsequent to Eq. (10)).

The price for this simplicity is that, in contrast to momentum subtraction schemes, the Appelquist-Carrazone decoupling theorem [9] does not hold. This is well-known in pure QCD where, at an energy scale μ, Green functions involving heavy quarks of mass m_h depend logarithmically on μ/m_h. In order to avoid potentially large logarithms for $\mu \ll m_h$ one has to decouple the heavy quark from the theory [10]. As a consequence, one obtains different coupling constants in the various energy regimes. They are connected by the so-called decoupling or matching relations. This is usually indicated by labeling α_s with a superscript which determines the number of active particles that contribute to its running. Considered as a function of μ, α_s shows a kink at one-loop and even a jump at higher orders when changing from one energy regime to the other.

The precise value where the heavy degrees of freedom are integrated out is not fixed by theory. Since the explicit dependence on this matching scale is logarithmic, it is natural to choose $\mu \approx m_h$. The dependence of theoretical predictions on the variation of the matching scale around this intuitive value can be used as an estimate of the theoretical uncertainty. Reduction of this uncertainty can only be achieved by means of higher order calculations.

Within QCD, the decoupling relations have been computed up to the three-loop order [11]. In the MSSM, only the one-loop relation for α_s is known [12,13]. It is the purpose of this paper to extend this calculation to two loops, such that a consistent three-loop evolution of α_s to the GUT scale can be performed. The matching coefficients that relate different energy regimes (with different values of n_s, n_f, and $n_{\tilde{g}}$) involve the masses of the heavy particles. Whereas at one-loop order the dependence is only logarithmic, it involves much more complicated functions at two-loop order. Furthermore, it is important whether the heavy particles have approximately similar masses and can thus be integrated out simultaneously, or whether the mass differences are big and the decoupling has to be performed step-by-step.

In this paper we will consider different scenarios concerning the hierarchy among the relevant particle masses. They are defined by the following conditions:

(A) $m_{\tilde{u}},\, \ldots,\, m_{\tilde{b}} \gg m_{\tilde{t}},\, m_{\tilde{g}},\, m_t \gg m_b$

(B) $m_{\tilde{u}},\, \ldots,\, m_{\tilde{b}},\, m_{\tilde{t}} \gg m_{\tilde{g}},\, m_t \gg m_b$

(C) $m_{\tilde{u}},\, \ldots,\, m_{\tilde{b}},\, m_{\tilde{t}},\, m_{\tilde{g}} \gg m_t \gg m_b$

(D) $m_{\tilde{u}},\, \ldots,\, m_{\tilde{b}},\, m_{\tilde{t}},\, m_{\tilde{g}},\, m_t \gg m_b\,,$

where $m_{\tilde{u}},\, \ldots,\, m_{\tilde{t}}$ are the squark masses, $m_{\tilde{g}}$ is the gluino mass and m_t, m_b are the top and the bottom quark mass, respectively.
In all cases it is understood that masses which are separated by a comma are of the same order of magnitude. Note that case (B) corresponds to so-called split SUSY which has been receiving much attention [14, 15] recently. Furthermore, in case (C) all supersymmetric masses are considered as heavy with respect to the SM ones. Squark masses are always taken to be larger than the top quark mass.

If all occurring mass scales are different, the resulting formulae are quite complicated and unhandy. For the purpose of this paper, we thus restrict ourselves to the simplified scenarios where either all masses are identified (if possible), or where an expansion in m_t/M can be performed, with $M \in \{m_{\tilde{u}}, \ldots, m_{\tilde{t}}, m_{\tilde{g}}\}$. Further details on our approximations will be given in Sections 3 and 5.

3 Technicalities

We follow the framework defined in Ref. [11, 16] (see also Ref. [17]) which reduces the calculation of the n-loop decoupling relation to n-loop vacuum diagrams. The bare decoupling (or matching) coefficients ζ_i^0, $\tilde{\zeta}_i^0$ are introduced as

$$\begin{aligned} g_s^{0\prime} &= \zeta_g^0 g_s^0 \,, \\ G_\mu^{0\prime,a} &= \sqrt{\zeta_3^0} G_\mu^{0,a} \,, \\ c^{0\prime,a} &= \sqrt{\tilde{\zeta}_3^0} c^{0,a} \,, \\ \Gamma_{ccg}^{0\prime} &= \tilde{\zeta}_1^0 \Gamma_{ccg}^0 \,, \end{aligned} \tag{1}$$

where $g_s = \sqrt{4\pi\alpha_s}$ is the QCD gauge coupling, G_μ^a is the gluon field, c^a is the Faddeev-Popov ghost field, and Γ_{ccg} is the ghost-gluon vertex. The prime generically denotes the quantities in the effective theory, where the heavy particles have been integrated out and the bare objects are marked by the superscript "0". According to Ref. [11], ζ_3^0, $\tilde{\zeta}_3^0$ and $\tilde{\zeta}_1^0$ are obtained from the gluon propagator, the ghost propagator, and the ghost-gluon vertex, all evaluated at vanishing external momenta. ζ_g^0 is then determined from the relation

$$\zeta_g^0 = \frac{\tilde{\zeta}_1^0}{\tilde{\zeta}_3^0 \sqrt{\zeta_3^0}} \,. \tag{2}$$

The renormalized decoupling coefficient is obtained with the help of the renormalization constants defined through

$$\begin{aligned} g_s^0 &= \mu^{2\epsilon} Z_g g_s \,, \\ G_\mu^{0,a} &= \sqrt{Z_3} G_\mu^a \,, \\ c^{0,a} &= \sqrt{\tilde{Z}_3} c^a \,, \\ \Gamma_{ccg}^0 &= \tilde{Z}_1 \Gamma_{ccg} \,, \end{aligned} \tag{3}$$

where μ is the renormalization scale and $D = 4 - 2\epsilon$ is the number of space-time dimensions. From Eq. (3) one obtains a relation that determines the renormalization constant of the strong coupling:

$$Z_g = \frac{\tilde{Z}_1}{\tilde{Z}_3 \sqrt{Z_3}} \,. \tag{4}$$

We have explicitly computed the two-loop expression for Z_g by evaluating Z_3, $\tilde{Z}_3$ and $\tilde{Z}_1$ to the corresponding order in the MSSM. The result will be given in Section 4.

The finite decoupling coefficient is obtained via

$$\zeta_g = \frac{Z_g}{Z_g'} \zeta_g^0 \,, \tag{5}$$

where Z_g' corresponds to the renormalization constant in the effective theory.

In Ref. [11, 17] the framework described above has been applied to the computation of the three-loop decoupling coefficients in QCD. The same method can be applied to the MSSM with the complication that more than one mass scale appears. In particular, one has to deal with a massive gluino and different masses for the two squarks of the same flavour. Furthermore, the different hierarchy structures among these masses lead to different expressions for the decoupling coefficients. The starting point of all scenarios defined in the Introduction is the energy regime where all particles of the theory are active (i.e., they contribute to the β function of the strong coupling); the corresponding coupling is denoted by $\alpha_s^{(\mathrm{full})}$. The end point is given by the regime where only the five lightest quark flavours are active, with the corresponding coupling denoted by $\alpha_s^{(5)}$. In case (D) a one-step decoupling from $\alpha_s^{(\mathrm{full})}$ to $\alpha_s^{(5)}$ is performed. However, in order to have more flexibility, in scenarios (A), (B) and (C) a two-step decoupling is defined where the corresponding strong couplings and decoupling coefficients are defined through

$$
\begin{array}{llcll}
\text{(A)} & \alpha_s^{(\tilde{t},\tilde{g},6)} = \left(\zeta_g^{\mathrm{A1}}\right)^2 \alpha_s^{(\mathrm{full})}\,, & & \alpha_s^{(5)} = \left(\zeta_g^{\mathrm{A2}}\right)^2 \alpha_s^{(\tilde{t},\tilde{g},6)}\,, \\
\text{(B)} & \alpha_s^{(\tilde{g},6)} = \left(\zeta_g^{\mathrm{B1}}\right)^2 \alpha_s^{(\mathrm{full})}\,, & & \alpha_s^{(5)} = \left(\zeta_g^{\mathrm{B2}}\right)^2 \alpha_s^{(\tilde{g},6)}\,, \\
\text{(C)} & \alpha_s^{(6)} = \left(\zeta_g^{\mathrm{C1}}\right)^2 \alpha_s^{(\mathrm{full})}\,, & & \alpha_s^{(5)} = \left(\zeta_g^{\mathrm{C2}}\right)^2 \alpha_s^{(6)}\,, \\
\text{(D)} & \alpha_s^{(5)} = \left(\zeta_g^{\mathrm{D}}\right)^2 \alpha_s^{(\mathrm{full})}\,. & &
\end{array}
\qquad (6)
$$

The dependence on the renormalization scale μ and — for the decoupling coefficients — on the masses is suppressed. The main goal of this paper is the computation of the ζ_g^X's.

Due to the isospin constraint between the top and bottom squark masses (see, e.g., Ref. [18]), scenario (A) is inconsistent. However, from the theoretical point of view it constitutes an appealing mass pattern. Furthermore, combined with scenario (C), it can be used to construct more realistic settings as will be described briefly at the end of Section 5. As our default scenario in the numerical discussion we adopt scenario (C).

Dimensional regularization (DREG) is the method which is most widely used in order to regularize the divergences of loop integrals. However, it is well-known that DREG violates supersymmetry. A possible compromise is provided by dimensional reduction (DRED) [19] which enforces the equality of fermionic and bosonic degrees of freedom while preserving all the calculational advantages of DREG. All the results of this paper are thus evaluated in the $\overline{\mathrm{DR}}$ scheme, i.e., we used DRED accompanied by minimal subtraction.

The final results are expressed in terms of the strong coupling constant α_s in the $\overline{\mathrm{DR}}$ scheme and the on-shell mass of quarks, squarks and gluinos. The experimental input, $\alpha_s(M_Z)$, is usually given in the $\overline{\mathrm{MS}}$ scheme, however, such that we need to convert it to the $\overline{\mathrm{DR}}$ scheme. We evaluated the corresponding relation through two loops in the MSSM, finding

$$
\alpha_s^{\overline{\mathrm{DR}}} = \alpha_s^{\overline{\mathrm{MS}}}\left[1+\frac{\alpha_s^{\overline{\mathrm{MS}}}}{\pi}\frac{C_A}{12}+\left(\frac{\alpha_s^{\overline{\mathrm{MS}}}}{\pi}\right)^2\left(\frac{11}{72}C_A^2-\frac{1}{16}C_A^2 n_{\tilde{g}}-\frac{1}{8}C_F T n_f\right)+\mathcal{O}(\alpha_s^3)\right], \qquad (7)
$$

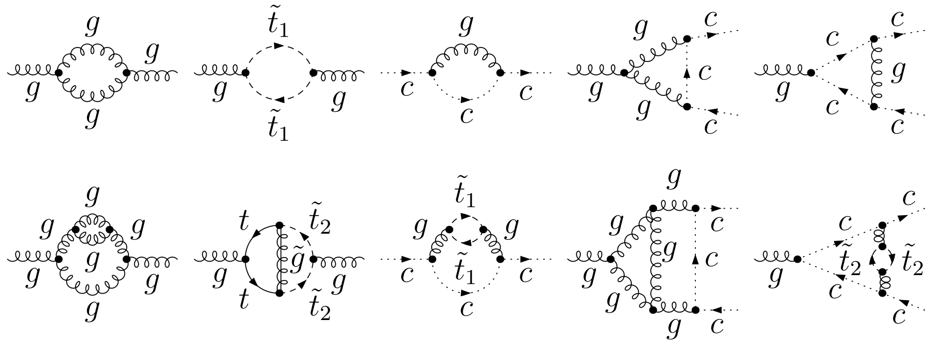

Figure 1: Sample diagrams contributing to Z_3, $\tilde{Z}_3$ and $\tilde{Z}_1$ with gluons (g), ghosts (c), top quarks (t), top squarks ($\tilde{t}$) and gluinos ($\tilde{g}$). The diagrams contributing to the decoupling coefficients must contain at least one heavy particle.

where n_f is the number of quark flavours and $n_{\tilde{g}} = 1$ or 0 distinguishes whether the gluino is active or not. Only the QCD-part of this equation will be used in what follows. It is obtained by setting $n_{\tilde{g}} = 0$ and agrees with Ref. [20]. With $n_f = 5$, the input $\alpha_s^{\overline{\rm MS}}(M_Z) = 0.1187 \pm 0.002$ [21] gives $\alpha_s^{\overline{\rm DR}}(M_Z) = 0.1198 \pm 0.002$ when using the one-loop approximation of Eq. (7), and $\alpha_s^{\overline{\rm DR}}(M_Z) = 0.1200 \pm 0.002$ with two-loop accuracy.

Note that, in what follows, we will often use the short hand notation

$$\alpha_s \equiv \alpha_s^{\overline{\rm DR}}(\mu)\,. \tag{8}$$

4 Renormalization constants and β function

In this section we present the results for the $\overline{\rm DR}$ renormalization constants. Since the $\overline{\rm DR}$ scheme is mass-independent, the calculation can be reduced to massless integrals depending on only one external momentum. More precisely, for Z_3, $\tilde{Z}_3$ and $\tilde{Z}_1$ one has to consider the gluon propagator, the ghost propagator, and the gluon-ghost vertex; in the latter case, the external momentum is chosen to flow through the ghost line. Sample diagrams are shown in Fig. 1. An important check is provided by the QCD result which we re-derive for general gauge parameter ξ, defined through the gluon propagator

$$D_g^{\mu\nu}(q) \quad = \quad -i\,\frac{g^{\mu\nu} - \xi\frac{q^\mu q^\nu}{q^2}}{q^2 + i\varepsilon}\,. \tag{9}$$

Up to two-loop order our results read [22]

$$
\begin{aligned}
Z_3 &= 1+\frac{\alpha_s}{\pi}\left\{\frac{1}{\epsilon}\left[C_A\left(\frac{5}{12}-\frac{n_{\tilde g}}{6}+\frac{\xi}{8}\right)-\frac{T}{6}(2n_f+n_s)\right]\right\} \\
&+\left(\frac{\alpha_s}{\pi}\right)^2\left\{\frac{1}{\epsilon^2}\left[C_A^2\left(-\frac{25}{192}+\frac{n_{\tilde g}}{96}(5-2\xi)+\frac{5\xi}{384}+\frac{\xi^2}{64}\right)+\frac{C_AT}{96}(2n_f+n_s)(5-2\xi)\right]\right. \\
&\quad+\frac{1}{\epsilon}\left[C_A^2\left(\frac{25}{128}-\frac{9}{64}n_{\tilde g}+\frac{15\xi}{256}-\frac{\xi^2}{128}\right)-\frac{C_FT}{8}(n_f+2n_s-n_sn_{\tilde g})\right. \\
&\quad\left.\left.-\frac{C_AT}{64}(10n_f-n_s-8n_sn_{\tilde g})\right]\right\}, \\
\tilde Z_3 &= 1+\frac{\alpha_s}{\pi}\left[\frac{1}{\epsilon}C_A\left(\frac{1}{8}+\frac{\xi}{16}\right)\right] \\
&+\left(\frac{\alpha_s}{\pi}\right)^2\left\{\frac{1}{\epsilon^2}\left[C_A^2\left(-\frac{1}{16}+\frac{1}{64}n_{\tilde g}-\frac{3\xi}{256}+\frac{3\xi^2}{512}\right)+C_AT(2n_f+n_s)\frac{1}{64}\right]\right. \\
&\quad\left.+\frac{1}{\epsilon}\left[C_A^2\left(\frac{43}{768}-\frac{5}{384}n_{\tilde g}-\frac{\xi}{512}\right)-C_AT(10n_f+11n_s)\frac{1}{384}\right]\right\}, \\
\tilde Z_1 &= 1+\frac{\alpha_s}{\pi}\left[\frac{1}{\epsilon}C_A\left(-\frac{1}{8}+\frac{\xi}{8}\right)\right] \\
&+\left(\frac{\alpha_s}{\pi}\right)^2\left[\frac{1}{\epsilon^2}C_A^2\left(\frac{5}{128}-\frac{7\xi}{128}+\frac{\xi^2}{64}\right)+\frac{1}{\epsilon}C_A^2\left(-\frac{3}{128}+\frac{7\xi}{256}-\frac{\xi^2}{256}\right)\right], \qquad (10)
\end{aligned}
$$

where n_f and n_s are the numbers of active quark and squark flavours, respectively, and $n_{\tilde g}=0$ or 1 distinguishes whether the gluino is active or not. For example, in the full MSSM it is $n_f=n_s=6$ and $n_{\tilde g}=1$. The terms involving $n_sn_{\tilde g}$ stem from diagrams containing a quark-squark-gluino vertex.[1] The precise meaning of α_s depends on the actual values of these constants. E.g., for $n_f=5$, $n_s=n_{\tilde g}=0$ it is $\alpha_s=\alpha_s^{(5)}$. For a gauge group SU(N_c), the colour factors in Eq. (10) are given by

$$
C_F=\frac{N_c^2-1}{2N_c}\,,\qquad C_A=N_c\,,\qquad T=1/2\,. \qquad (11)
$$

The combination of Z_3, $\tilde Z_3$ and $\tilde Z_1$ according to Eq. (4) leads to the renormalization

[1]Note that in this paper $\tilde q_L$, $\tilde q_R$ are either both active or both integrated out. Also, we always assume that, if $\tilde q$ is active, so is q ($q\in\{u,d,c,s,t,b\}$).

constant for the strong coupling

$$
\begin{aligned}
(Z_g)^2 &= 1+\frac{\alpha_s}{\pi}\cdot\frac{1}{\epsilon}\left[C_A\left(-\frac{11}{12}+\frac{1}{6}n_{\tilde g}\right)+\frac{T}{6}(2n_f+n_s)\right]\\
&\quad+\left(\frac{\alpha_s}{\pi}\right)^2\left\{\frac{1}{\epsilon^2}\left[C_A^2\left(-\frac{121}{144}-\frac{5}{18}n_{\tilde g}\right)+\frac{T^2}{36}(2n_f+n_s)^2\right]\right.\\
&\quad\quad+\frac{1}{\epsilon}\left[C_A^2\left(-\frac{17}{48}+\frac{1}{6}n_{\tilde g}\right)+\frac{C_FT}{8}(n_f+2n_s-n_sn_{\tilde g})\right.\\
&\quad\quad\left.\left.+\frac{C_AT}{24}(5n_f+n_s-3n_sn_{\tilde g})\right]\right\} \qquad (12)
\end{aligned}
$$

which is needed for the renormalization of the decoupling coefficient (cf. Eq. (5)).

From Z_g one obtains the β function defined through

$$
\mu^2\frac{\mathrm{d}}{\mathrm{d}\mu^2}\frac{\alpha_s}{\pi} = \beta(\alpha_s) = -\left(\frac{\alpha_s}{\pi}\right)^2\sum_{i\ge0}\beta_i\left(\frac{\alpha_s}{\pi}\right)^i, \qquad (13)
$$

with the result

$$
\begin{aligned}
\beta_0 &= \frac{1}{4}\left[C_A\left(\frac{11}{3}-\frac{2}{3}n_{\tilde g}\right)-\frac{2}{3}T(n_s+2n_f)\right], \qquad (14)\\
\beta_1 &= \frac{1}{16}\left[C_A^2\left(\frac{34}{3}-\frac{16}{3}n_{\tilde g}\right)-\frac{4}{3}C_AT(5n_f+n_s-3n_sn_{\tilde g})-4C_FT(n_f+2n_s-n_sn_{\tilde g})\right].
\end{aligned}
$$

Note that due to the terms $\propto n_sn_{\tilde g}$ this result can also be used for scenarios where the gluino is decoupled but (some) squarks are not. However, for the three-loop coefficient β_2 (see below) such terms are not separately available. Thus in the following we identify $n_sn_{\tilde g}\to n_s$.

The results for β_0 and β_1 are renormalization scheme independent. The pure QCD part agrees with the well-known $\overline{\rm MS}$ result which can be found in Ref. [23], for example. The contribution from the SUSY particles agrees with Ref. [24].

The two-loop decoupling relations presented in the next section have to be used in conjunction with the three-loop coefficient of the β function. Subtracting the pure QCD result in the $\overline{\rm DR}$ scheme [20] from the fully supersymmetric expression [24], we can distinguish the contributions from squarks and gluinos and multiply them by the appropriate labels n_s and $n_{\tilde g}$:

$$
\begin{aligned}
\beta_2 &= \frac{1}{64}\left[C_A^3\left(\frac{3115}{54}-\frac{1981}{54}n_{\tilde g}\right)+C_A^2T\left(\frac{899}{27}n_s-\frac{1439}{27}n_f\right)+C_AT^2\left(-\frac{50}{27}n_s^2+\frac{158}{27}n_f^2\right)\right.\\
&\left.-C_AC_FT\left(\frac{209}{9}n_s+\frac{259}{9}n_f\right)+C_F^2T\left(14n_s+2n_f\right)+C_FT^2\left(\frac{148}{9}n_s^2+\frac{68}{9}n_f^2\right)\right]. \qquad (15)
\end{aligned}
$$

Note that since Ref. [24] assumed $n_f = n_s$, it is not possible to distinguish the term proportional to $n_s n_f$ from the n_s^2 term. For this reason, Eq. (15) can only be used for $n_f = n_s$ or $n_s = 0$; unfortunately, this prevents us from discussing scenario (A) in the numerical applications. As expected, the pure QCD result in $\overline{\mathrm{DR}}$, obtained by setting $n_s = n_{\tilde{g}} = 0$ in Eq. (15), is different from the expression in the $\overline{\mathrm{MS}}$ scheme; only the coefficients of the colour structures $C_A T^2 n_f^2$ and $C_F^2 T n_f$ are the same in both schemes.

Apart from the $\overline{\mathrm{DR}}$ renormalization constants in Eq. (10), we also need the one-loop renormalization constants for the top quark and squark mass. The explicit on-shell expressions are given in Eqs. (B.5) and (B.6) of Ref. [13]. The on-shell counterterm for the gluino mass reads (see, e.g., Ref. [25])

$$\begin{aligned}
\frac{m_{\tilde{g}}^B}{m_{\tilde{g}}} &= 1 - \frac{\alpha_s}{\pi}\Bigg\{ \frac{1}{4\epsilon}(3C_A - 2Tn_s) + \frac{1}{2}C_A\left(\frac{5}{2} + \frac{3}{2}L_{\tilde{g}}\right) \\
&\quad + T\sum_q \sum_{i=1}^{2} \frac{1}{4}\left[\frac{m_q^2}{m_{\tilde{g}}^2}(1+L_q) - \frac{m_{\tilde{q}_i}^2}{m_{\tilde{g}}^2}(1+L_{\tilde{q}_i}) + \frac{m_{\tilde{q}_i}^2 - m_{\tilde{g}}^2 - m_q^2}{m_{\tilde{g}}^2} B_0^{\mathrm{fin}}(m_{\tilde{g}}^2, m_q, m_{\tilde{q}_i})\right] \\
&\quad - T\sum_q \frac{1}{2}\frac{m_q}{m_{\tilde{g}}}\sin 2\theta_q \left[B_0^{\mathrm{fin}}(m_{\tilde{g}}^2, m_q, m_{\tilde{q}_1}) - B_0^{\mathrm{fin}}(m_{\tilde{g}}^2, m_q, m_{\tilde{q}_2})\right]\Bigg\}\,, \qquad (16)
\end{aligned}$$

where B_0^{fin} is defined in Eq. (B.8) of Ref. [13]. Note that the $\mathcal{O}(\epsilon)$ part of the mass counterterms is not needed since the one-loop result depends only logarithmically on the masses. In Eq. (16), we have used the short-hand notation

$$L_x = \ln\frac{\mu^2}{m_x^2}\,, \qquad x \in \{q,\, t,\, \tilde{g},\, \tilde{q}_i,\, \ldots\}\,. \qquad (17)$$

In addition to that, the abbreviations

$$L_{\tilde{M}} = \ln\frac{\mu^2}{\tilde{M}^2}\,, \qquad L_{\tilde{m}} = \ln\frac{\mu^2}{\tilde{m}^2}\,, \qquad L_{t\tilde{m}} = \ln\frac{m_t^2}{\tilde{m}^2}\,, \qquad (18)$$

will be used in what follows.

5 Decoupling coefficients

As already pointed out in Section 3, the calculation of the decoupling coefficients can be reduced to vacuum integrals [11,16,17]. At two-loop level, such integrals can be evaluated fully analytically [26] for arbitrary masses. For the purpose of this paper, however, it is sufficient to solve them for either a single or for two largely separated mass scales. In the first case, the analytical result is rather short in general, while in the second case we can perform an asymptotic expansion in the ratio of the two mass scales and truncate the series after the first few terms which leads again to a fairly compact expression. Furthermore, in order to shorten the expressions even more, we present the results for the SU(3) gauge group.

The Feynman diagrams are generated using `QGRAF` [27], and subsequently translated by `Q2E/EXP` [28, 29] to the notation of `MATAD` [30], which evaluates the vacuum integrals. If the integrals contain more than one mass scale, `EXP` performs an asymptotic expansion on the diagrams before passing them on to `MATAD`.

Before discussing the different scenarios, we present the pure QCD result for ζ_g in the $\overline{\rm DR}$ scheme, where the top quark is considered as heavy and the remaining $(n_f - 1) = 5$ quarks are massless. Up to two-loop order, the decoupling coefficient relating $\alpha_s^{(n_f)}$ and $\alpha_s^{(n_f-1)}$ via

$$\alpha_s^{(n_f-1)} = (\zeta_g^{\rm QCD})^2 \alpha_s^{(n_f)} \tag{19}$$

reads

$$(\zeta_g^{\rm QCD})^2 = 1 - \frac{\alpha_s^{(n_f)}}{\pi}\frac{1}{6}L_t + \left(\frac{\alpha_s^{(n_f)}}{\pi}\right)^2 \left(-\frac{5}{24} - \frac{19}{24}L_t + \frac{1}{36}L_t^2\right) + \mathcal{O}\left(\alpha_s^3\right) , \tag{20}$$

with $L_t = \ln(\mu^2/m_t^2)$. Note that in the $\overline{\rm MS}$ scheme the constant term of order α_s^2 is $-7/24$ instead of $-5/24$ as in Eq. (20) [10, 11, 16, 31]. The transformation of Eq. (19) from the $\overline{\rm DR}$ to the $\overline{\rm MS}$ scheme confirms the fermionic two-loop coefficient of Eq. (7).

Within the MSSM, the one-loop result for the decoupling coefficient relating $\alpha_s^{(5)}$ to the strong coupling where also squarks and gluinos are active can be written in the generic form (see, e.g., Ref. [13])

$$\begin{aligned}(\zeta_g^{\rm SUSY})^2 &= 1 + \frac{\alpha_s^{\rm (SUSY)}}{\pi}\Bigg[-\frac{1}{6}L_t - \frac{1}{12}\sum_{s=1}^{n_s} L_{\tilde{q}_s} - \frac{n_{\tilde{g}}}{2}L_{\tilde{g}} - \epsilon\Bigg(\frac{1}{12}\left(\zeta(2)+L_t^2\right) \\ &\quad + \frac{1}{24}\sum_{s=1}^{n_s}\left(\zeta(2)+L_{\tilde{q}_s}^2\right) + \frac{n_{\tilde{g}}}{4}\left(\zeta(2)+L_{\tilde{g}}^2\right)\Bigg)\Bigg] + \mathcal{O}\left(\alpha_s^2\right) ,\end{aligned} \tag{21}$$

with the notation as defined in Eqs. (17) and (18), and $\zeta(2) = \pi^2/6 = 1.64493\ldots$. For the sake of consistency, also the term of order ϵ is given; it is needed in intermediate steps of the calculation. The sum runs over all active squark flavours. We introduced a generic label "SUSY" which has to be adapted to the scenarios (A)–(D) discussed above. Note that due to the different mass scales involved in Eq. (21), α_s exhibits a jump even at one-loop order if all heavy particles are integrated out at the same scale.

Let us now discuss the various cases defined in the Introduction and in Eq. (6). The common large mass will be denoted by $\tilde{M}$ and the common smaller mass by $\tilde{m}$. In some cases, the SUSY masses will be taken to be (much) larger than the top quark mass. However, it turns out that the expansion in the ratio converges very fast — even for equal masses. Since in Section 6 the inverse decoupling coefficients are needed, we will give explicit results for them. The analytic expressions for ζ_g itself can be obtained easily by recursive substitution of the one-loop relations.

5.1 Scenario (A)

$$m_{\tilde{u}} = \ldots = m_{\tilde{b}} = \tilde{M} \quad \gg \quad \tilde{m} = m_{\tilde{t}} = m_{\tilde{g}}\,,\ m_t$$
$$\alpha_s^{(\tilde{t},\tilde{g},6)} = (\zeta_g^{\rm A1})^2\,\alpha_s^{(\rm full)}\,, \qquad \alpha_s^{(5)} = (\zeta_g^{\rm A2})^2\,\alpha_s^{(\tilde{t},\tilde{g},6)}$$

$\zeta_g^{\rm A1}$ is a function of $\tilde{M}$ only. In fact, following the method of Ref. [11,16,17], the masses of the gluino, the top squarks and all quarks have to be set to zero in the corresponding Feynman diagrams,[2] cf. Fig. 1. The result is

$$\frac{1}{(\zeta_g^{\rm A1})^2} \;=\; 1 + \frac{\alpha_s^{(\tilde{t},\tilde{g},6)}}{\pi}\frac{n_s}{12}L_{\tilde{M}} + \left(\frac{\alpha_s^{(\tilde{t},\tilde{g},6)}}{\pi}\right)^2\left(-\frac{13}{48}n_s - \frac{n_s}{12}L_{\tilde{M}} + \left(\frac{n_s}{12}L_{\tilde{M}}\right)^2\right)\,, \tag{22}$$

with $n_s = 5$.

The Feynman diagrams leading to $\zeta_g^{\rm A2}$ do not contain the five squark flavours already integrated out in step A1. However, one has the top squarks, gluino and top quark as massive. We consider two limits:

(A2a) $\tilde{m} = m_t$:

$$\begin{aligned}\frac{1}{(\zeta_g^{\rm A2a})^2} &= 1 + \frac{\alpha_s^{(5)}}{\pi}\frac{3}{4}L_{\tilde{m}} \\ &\quad + \left(\frac{\alpha_s^{(5)}}{\pi}\right)^2\left(\frac{1909}{864} + \frac{11\sqrt{3}}{108}\pi + \frac{17}{12}S_2 + \frac{89}{24}L_{\tilde{m}} + \left(\frac{3}{4}L_{\tilde{m}}\right)^2\right)\,,\end{aligned} \tag{23}$$

(A2b) $\tilde{m} \gg m_t$:

$$\begin{aligned}\frac{1}{(\zeta_g^{\rm A2b})^2} &= 1 + \frac{\alpha_s^{(5)}}{\pi}\left(\frac{1}{6}L_t + \frac{7}{12}L_{\tilde{m}}\right) \\ &\quad + \left(\frac{\alpha_s^{(5)}}{\pi}\right)^2\Bigg[\frac{265}{96} + \frac{19}{24}L_t + \frac{35}{12}L_{\tilde{m}} + \left(\frac{1}{6}L_t + \frac{7}{12}L_{\tilde{m}}\right)^2 \\ &\quad + \left(\frac{m_t}{\tilde{m}}\right)^2\left(-\frac{5}{48} - \frac{3}{8}L_{t\tilde{m}}\right) + \frac{7\pi}{36}\left(\frac{m_t}{\tilde{m}}\right)^3 \\ &\quad + \left(\frac{m_t}{\tilde{m}}\right)^4\left(-\frac{881}{7200} + \frac{1}{80}L_{t\tilde{m}}\right) - \frac{7\pi}{288}\left(\frac{m_t}{\tilde{m}}\right)^5 + \ldots\Bigg]\,,\end{aligned} \tag{24}$$

where $S_2 = \frac{4}{9\sqrt{3}}{\rm Cl}_2(\frac{\pi}{3}) \simeq 0.260434$. It is interesting to note that $1/(\zeta_g^{\rm A2b})^2$ as given in Eq. (24) evaluated for $\tilde{m} = m_t$ approximates $1/(\zeta_g^{\rm A2a})^2$ to an accuracy better than 1%.

[2]Note that this is no restriction on the resulting effective theory: once the heavy particles are decoupled, the remaining fields can have arbitrary masses $\ll \tilde{M}$.

5.2 Scenario (B)

$$m_{\tilde{u}} = \ldots = m_{\tilde{t}} = \tilde{M} \quad \gg \quad m_{\tilde{g}}\,,\ m_t$$
$$\alpha_s^{(\tilde{g},6)} = (\zeta_g^{\mathrm{B1}})^2\,\alpha_s^{(\mathrm{full})}\,, \qquad \alpha_s^{(5)} = (\zeta_g^{\mathrm{B2}})^2\,\alpha_s^{(\tilde{g},6)}$$

The analytical expression for ζ_g^{B1} is identical to the one of ζ_g^{A1}, only now we have $n_s = 6$. In the case of ζ_g^{B2} there is no gluino-top-stop interaction since at this stage all squarks are already integrated out. As a consequence the integrations factorize into parts where either the gluino or the top quark is the only massive particle. One obtains

$$\begin{aligned}\frac{1}{(\zeta_g^{\mathrm{B2}})^2} &= 1 + \frac{\alpha_s^{(5)}}{\pi}\left(\frac{1}{6}L_t + \frac{1}{2}L_{\tilde{g}}\right)\\ &+ \left(\frac{\alpha_s^{(5)}}{\pi}\right)^2\left[\frac{275}{96} + \frac{19}{24}L_t + 3L_{\tilde{g}} + \left(\frac{1}{6}L_t + \frac{1}{2}L_{\tilde{g}}\right)^2\right]\,. \end{aligned} \tag{25}$$

5.3 Scenario (C)

$$m_{\tilde{u}} = \ldots = m_{\tilde{t}} = m_{\tilde{g}} = \tilde{M} \quad \gg \quad m_t$$
$$\alpha_s^{(6)} = (\zeta_g^{\mathrm{C1}})^2\,\alpha_s^{(\mathrm{full})}\,, \qquad \alpha_s^{(5)} = (\zeta_g^{\mathrm{C2}})^2\,\alpha_s^{(6)}$$

The result for ζ_g^{C1} is given by

$$\begin{aligned}\frac{1}{(\zeta_g^{\mathrm{C1}})^2} &= 1 + \frac{\alpha_s^{(6)}}{\pi}\left(\frac{1}{2} + \frac{n_s}{12}\right)L_{\tilde{M}}\\ &+ \left(\frac{\alpha_s^{(6)}}{\pi}\right)^2\left[\frac{85}{32} - \frac{5}{48}n_s + \left(3 - \frac{n_s}{12}\right)L_{\tilde{M}} + \left(\frac{1}{2} + \frac{n_s}{12}\right)^2 L_{\tilde{M}}^2\right]\,, \end{aligned} \tag{26}$$

with $n_s = 6$. ζ_g^{C2} is identical to the pure QCD result of Eq. (20),

$$\zeta_g^{\mathrm{C2}} = \zeta_g^{\mathrm{QCD}}\,. \tag{27}$$

5.4 Scenario (D)

$$\tilde{M} = m_{\tilde{u}} = \ldots = m_{\tilde{t}} = m_{\tilde{g}}\,,\ m_t$$
$$\alpha_s^{(5)} = (\zeta_g^{\mathrm{D}})^2\,\alpha_s^{(\mathrm{full})}$$

As in the case (A2) we consider two limits:

<u>(Da) $\tilde{M} = m_t$:</u>

$$\begin{aligned}\frac{1}{\left(\zeta_g^{\mathrm{Da}}\right)^2} &= 1 + \frac{\alpha_s^{(5)}}{\pi}\left(\frac{2}{3} + \frac{n_s}{12}\right)L_{\tilde{M}} + \left(\frac{\alpha_s^{(5)}}{\pi}\right)^2\left[\frac{1999}{864} + \frac{11\sqrt{3}}{108}\pi + \frac{17}{12}S_2 - \frac{5}{48}n_s\right.\\ &\left. + \left(\frac{91}{24} - \frac{n_s}{12}\right)L_{\tilde{M}} + \left(\frac{2}{3} + \frac{n_s}{12}\right)^2 L_{\tilde{M}}^2\right]\,, \end{aligned} \tag{28}$$

(Db) $\tilde{M} \gg m_t$:

$$\frac{1}{\left(\zeta_g^{\rm Db}\right)^2} = 1 + \frac{\alpha_s^{(5)}}{\pi}\left[\frac{1}{6}L_t + \left(\frac{1}{2}+\frac{n_s}{12}\right)L_{\tilde{M}}\right] + \left(\frac{\alpha_s^{(5)}}{\pi}\right)^2\left\{\frac{275}{96} - \frac{5}{48}n_s + \frac{19}{24}L_t\right.$$
$$+\left(3-\frac{n_s}{12}\right)L_{\tilde{M}} + \left[\frac{1}{6}L_t + \left(\frac{1}{2}+\frac{n_s}{12}\right)L_{\tilde{M}}\right]^2$$
$$+\left(\frac{m_t}{\tilde{M}}\right)^2\left(-\frac{5}{48}-\frac{3}{8}L_{t\tilde{m}}\right) + \frac{7\pi}{36}\left(\frac{m_t}{\tilde{M}}\right)^3$$
$$\left.+\left(\frac{m_t}{\tilde{M}}\right)^4\left(-\frac{881}{7200}+\frac{1}{80}L_{t\tilde{m}}\right) - \frac{7\pi}{288}\left(\frac{m_t}{\tilde{M}}\right)^5 + \ldots\right\}, \tag{29}$$

where we have $n_s = 6$ in both cases. We again observe very good convergence of $1/\left(\zeta_g^{\rm Db}\right)^2$ even for $\tilde{M} = m_t$; thus, for our numerical analysis in Section 6 we only take the result from Eq. (29).

At this point two remarks are in order. First, it is interesting to note that the following relation holds:

$$\zeta^{\rm C1}\zeta^{\rm C2} \;=\; \zeta^{\rm Db} + \mathcal{O}\left(\frac{m_t^2}{\tilde{M}^2}\right), \tag{30}$$

which constitutes an important cross check of our calculation. Second, let us remark that it is possible to add the terms of $\zeta_g^{\rm C1}$ involving n_s to $\zeta_g^{\rm A2a}$ or $\zeta_g^{\rm A2b}$ and thus take into account additional squarks as being integrated out together with the top squark, gluino and top quark. Of course, the parameter n_s of $\zeta_g^{\rm A1}$ has to be adjusted accordingly.

6 Numerics

In this section we study the phenomenological implications of the two-loop decoupling coefficients. In particular, we compute the value of the strong coupling $\alpha_s^{(\rm full)}(M_{\rm SUSY})$ at a high scale $M_{\rm SUSY}$, as evolved from the experimental input value $\alpha_s^{(5)}(M_Z)$. As described in Section 2, at higher orders in perturbation theory heavy particles have to be decoupled properly when crossing the corresponding particle threshold. However, the precise value of the scale where this is done, $\mu_{\rm th}$, is not fixed by theory and can be used as a means to estimate the theoretical uncertainty. On general grounds one expects that, at fixed order perturbation theory, the relation between $\alpha_s^{(5)}(M_Z)$ and $\alpha_s^{(\rm full)}(M_{\rm SUSY})$ is not very sensitive to the choice of the matching scale as long as $\mu_{\rm th}$ is of the order of the heavy mass scale. In the following we study $\alpha_s^{(\rm full)}(M_{\rm SUSY})$ as a function of $\mu_{\rm th}$ for the first three orders in perturbation theory.

Let us describe the procedure for computing $\alpha_s^{(\rm full)}(M_{\rm SUSY})$ from the knowledge of $\alpha_s^{(5)}(M_Z)$ in detail for scenario (C); the other cases can be treated in complete analogy.

μ	$\alpha_s(\mu)$
800 GeV	0.0916 ± 0.0012
μ_{GUT}	0.0398 ± 0.00023

Table 1: $\alpha_s(\mu)$ in the $\overline{\mathrm{DR}}$ scheme for $\mu = 800$ GeV and $\mu = \mu_{\mathrm{GUT}}$ assuming scenario (C). The starting point for the prescription described above Eq. (31) is defined in Eq. (32). The error is due to the experimental uncertainty of $\alpha_s(M_Z)$.

First, we compute $\alpha_s^{(5)}(\mu_{\mathrm{th}}^{\mathrm{C2}})$ from $\alpha_s^{(5)}(M_Z)$ by using the L-loop β function with $n_f = 5$ and $n_s = n_{\tilde{g}} = 0$, and numerically solving the corresponding renormalization group equation. In the next step, the $(L-1)$-loop expression of ζ_g^{C2} is used to arrive at $\alpha_s^{(6)}(\mu_{\mathrm{th}}^{\mathrm{C2}})$. With the help of the L-loop β function (with $n_f = 6$, $n_s = 0$ and $n_{\tilde{g}} = 0$) we then evaluate $\alpha_s^{(6)}(\mu_{\mathrm{th}}^{\mathrm{C1}})$ and perform the matching to $\alpha_s^{(\mathrm{full})}(\mu_{\mathrm{th}}^{\mathrm{C1}})$ using ζ_g^{C1} at $(L-1)$-loop order. Finally, $\alpha_s^{(\mathrm{full})}(M_{\mathrm{SUSY}})$ is obtained again with the help of the L-loop β function after setting $n_f = 6$, $n_s = 6$ and $n_{\tilde{g}} = 1$. We apply this procedure for $L = 1$, 2 and 3 and study the dependence on the two matching scales $\mu_{\mathrm{th}}^{\mathrm{C1}}$ and $\mu_{\mathrm{th}}^{\mathrm{C2}}$. Of course, in scenario (D) there is only one matching scale and the procedure simplifies accordingly.

Before discussing the numerical effects, let us specify the input values used in our analysis. In the four scenarios defined in Section 2 we need to define a large and a small mass scale, $\tilde{M}$ and $\tilde{m}$, and the top quark mass. We choose

$$\begin{aligned} m_t &= 174 \text{ GeV}\,, \\ \tilde{M} &= 1000 \text{ GeV}\,, \\ \tilde{m} &= 400 \text{ GeV}\,. \end{aligned} \tag{31}$$

For the default values of the matching scales we assume $\mu_{\mathrm{th},1} = \tilde{M}$ and $\mu_{\mathrm{th},2} = \tilde{m}$. Furthermore, according to the discussion below Eq. (7), we use

$$\alpha_s^{(5)}(M_Z) = 0.120 \pm 0.002\,, \tag{32}$$

where the label $\overline{\mathrm{DR}}$ has again been omitted. The GUT scale will be taken as $\mu_{\mathrm{GUT}} = 10^{16}$ GeV.

In order to get an impression of the numerical value for α_s at various scales and the uncertainties induced by the input $\alpha_s(M_Z)$, Tab. 1 gives $\alpha_s(\mu)$ for $\mu = 800$ GeV and $\mu = \mu_{\mathrm{GUT}}$. These numbers are obtained from Eq. (32) for scenario (C) with three-loop running and two-loop matching. Further on, the dependence on the matching scales and the loop order is exemplified in Fig. 2 which shows $\alpha_s(\mu_{\mathrm{GUT}})$ for scenario (C) as a function of $\mu_{\mathrm{th},1}$ and $\mu_{\mathrm{th},2}$, each of them varying by a factor of ten around its default value. One can clearly see how the result stabilizes as soon as two-loop running and one-loop matching (middle plane) is included. The three-loop corrections stabilize the dependence of α_s on $\mu_{\mathrm{th},1}$ and $\mu_{\mathrm{th},2}$ even more (upper plane), such that the result is practically independent of

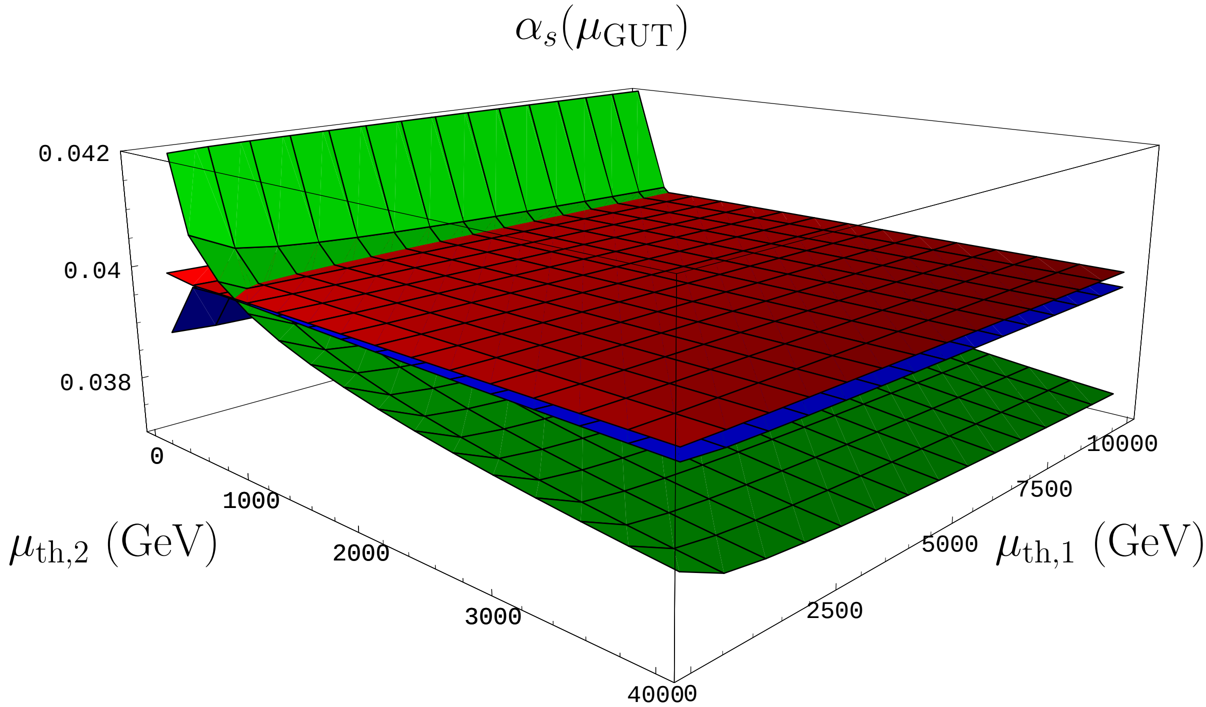

Figure 2: $\alpha_s(\mu_{\rm GUT})$ for $\mu_{\rm GUT} = 10^{16}$ GeV as a function of the two matching scales $\mu_{\rm th,1}$ and $\mu_{\rm th,2}$. The lower (green), middle (blue) and upper (red) planes correspond to one-, two- and three-loop running accompanied with the corresponding order in the decoupling relation for the scenario (C).

the matching scales within a wide range around their default values. Within the considered range of $\mu_{\rm th,1}$ and $\mu_{\rm th,2}$, the variation of $\alpha_s(\mu_{\rm GUT})$ is 13.8/1.6/0.3% at 1-/2-/3-loop order.

Figs. 3 and 4 show the dependence on one of the scales when the other is kept at its default value. In scenario (D), where only one matching scale is present, we set all SUSY masses to $\tilde{M}$ when the variation of $\mu_{\rm th,1}$ is considered (Fig. 3), and to $\tilde{m}$ when $\mu_{\rm th,2}$ is varied (Fig. 4). A drastic improvement can be observed after including two-loop running and one-loop matching. When the three-loop running is included, the scale variation becomes almost completely flat.

In order to study the effect of different mass configurations, Figs. 5(a) and (b) compare the three-loop curves of Figs. 3 and 4 among scenarios (B)–(D) (long to short dashes). One observes differences of the order 0.005 which is about a factor 10 larger than the uncertainty originating from the current experimental uncertainty in $\alpha_s(M_Z)$. Estimating the theoretical uncertainty by the difference between the two- and three-loop result, we obtain

$$\alpha_s(\mu_{\rm GUT}) = 0.0398 \pm 0.00023\Big|_{\delta\alpha_s(M_Z)} \pm 0.0025\Big|_{\rm masses} \pm 0.00007\Big|_{\rm th} . \tag{33}$$

Another practical application of our results is shown in Fig. 6, where the strong cou-

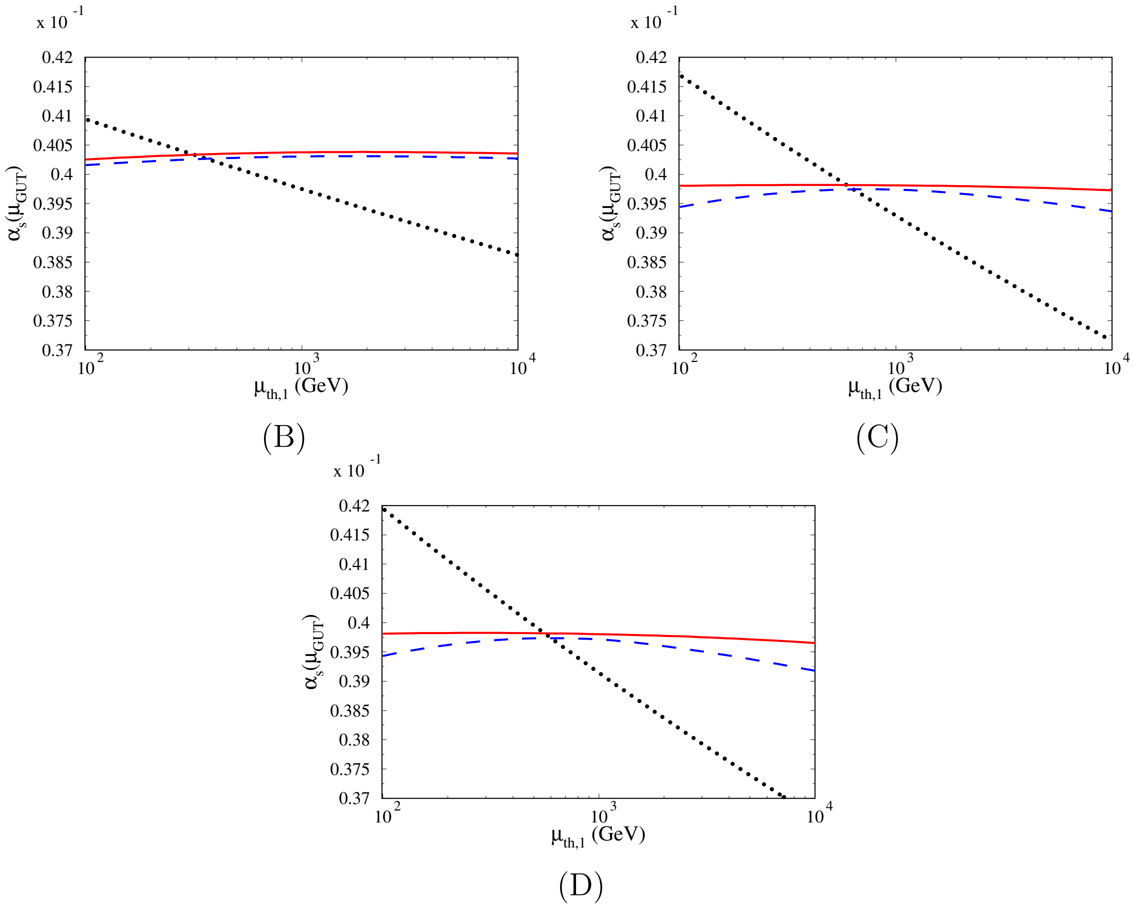

Figure 3: $\alpha_s(\mu_{\rm GUT})$ as a function of $\mu_{\rm th,1}$ for scenario (B)–(D). The dotted, dashed and full lines correspond to one-, two- and three-loop running. In scenario (D) we set all SUSY masses to $\tilde{M}$.

pling at a proposed center-of-mass energy $\sqrt{s} = 800$ GeV of a future International Linear Collider (ILC) is computed. While for $\mu_{\rm th,2} \approx 200$ GeV the two- and three-loop result practically give the same value for α_s, for $\mu_{\rm th,2} = 2000$ GeV the shift induced by the new three-loop terms is comparable with the uncertainty induced by the experimental value for $\alpha_s(M_Z)$ (cf. Tab. 1). This underlines once more the importance of the two-loop decoupling and three-loop running terms.

Fig. 7(a) shows $1/\alpha_s$ as a function of μ from the weak to the Planck scale, $\mu_{\rm PL} = 10^{19}$ GeV, where the dotted, dashed and solid lines correspond to one-, two- and three-loop running. It can be seen that there are kinks at 400 GeV and 1000 GeV where the slope of the curves changes. A closer look shows that the two- and three-loop curves actually are discontinuous as α_s jumps due to the one- and two-loop decoupling relations. In this plot the uncertainties from $\alpha_s(M_Z)$ or the various mass patterns of the supersymmetric particles are hardly visible. For this reason, we show in Fig. 7(b) the ratio $\alpha_s(\mu)/\alpha_{s,0}(\mu)$, where $\alpha_{s,0}(\mu)$ is the leading order result for scenario (C) with $\alpha_{s,0}(M_Z) = 0.120$. The

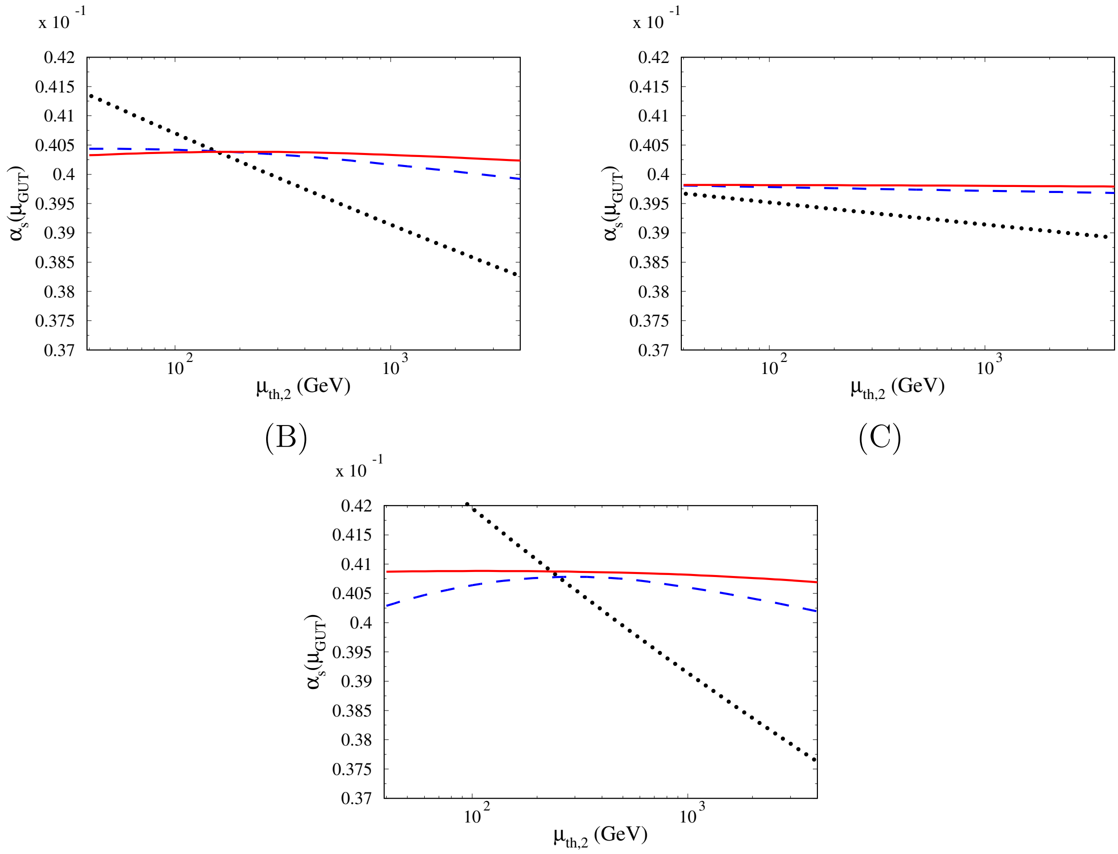

(D)

Figure 4: $\alpha_s(\mu_{\rm GUT})$ as a function of $\mu_{\rm th,2}$ for scenario (B)–(D). The dotted, dashed and full lines correspond to one-, two- and three-loop running. In scenario (D) we set all SUSY masses to $\tilde{m}$.

scale μ is varied between M_Z and $\mu_{\rm PL}$. The dotted, dashed, and solid line correspond to the one-, two-, and three-loop result of scenario (C), respectively, Note that below $\mu_{\rm th,2} = \tilde{m} = 400$ GeV the difference between the dashed and full curve is very small. The (green) band indicates the variation originating from the experimental uncertainty of $\alpha_s^{\overline{\rm DR}}(M_Z)$ (cf. Eq. (32)). The dash-dotted lines correspond to the three-loop results of scenario (D) where the masses are set to $2\tilde{M}$ (lower) and $\tilde{m}$ (upper), respectively. They thus reflect the dependence on the mass parameters of the MSSM. The corresponding curve for scenario (B) would lie between the two dash-dotted lines and are therefore not shown.

In Fig. 8 we combine our three-loop accuracy findings for the evolution of the inverse strong coupling at the GUT scale (yellow band) with the two-loop order results for the strong (α_s, red band), the electro-magnetic (α_1, blue band) and the weak coupling (α_2, green band) (for a precise definition, see Ref. [7], and references therein). The wide error bands correspond to the present experimental accuracy for the gauge couplings and the

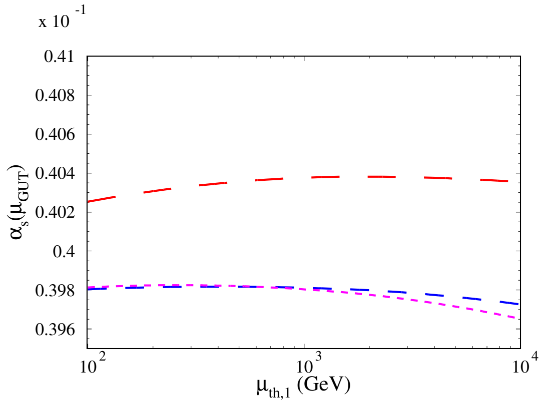

(a)

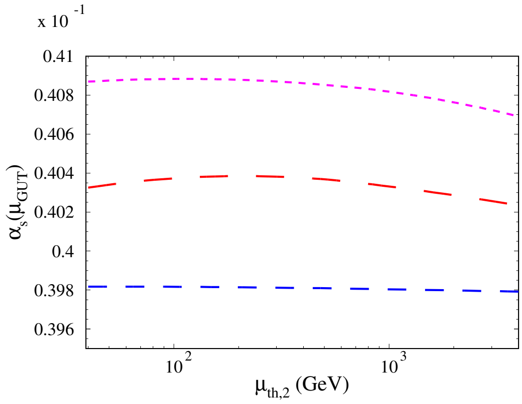

(b)

Figure 5: Comparison of $\alpha_s(\mu_{\rm GUT})$ as a function of $\mu_{\rm th,1}$ (a) and $\mu_{\rm th,2}$ (b) where for the cases (B), (C) and (D) (from long to short dashes) the three-loop results are plotted.

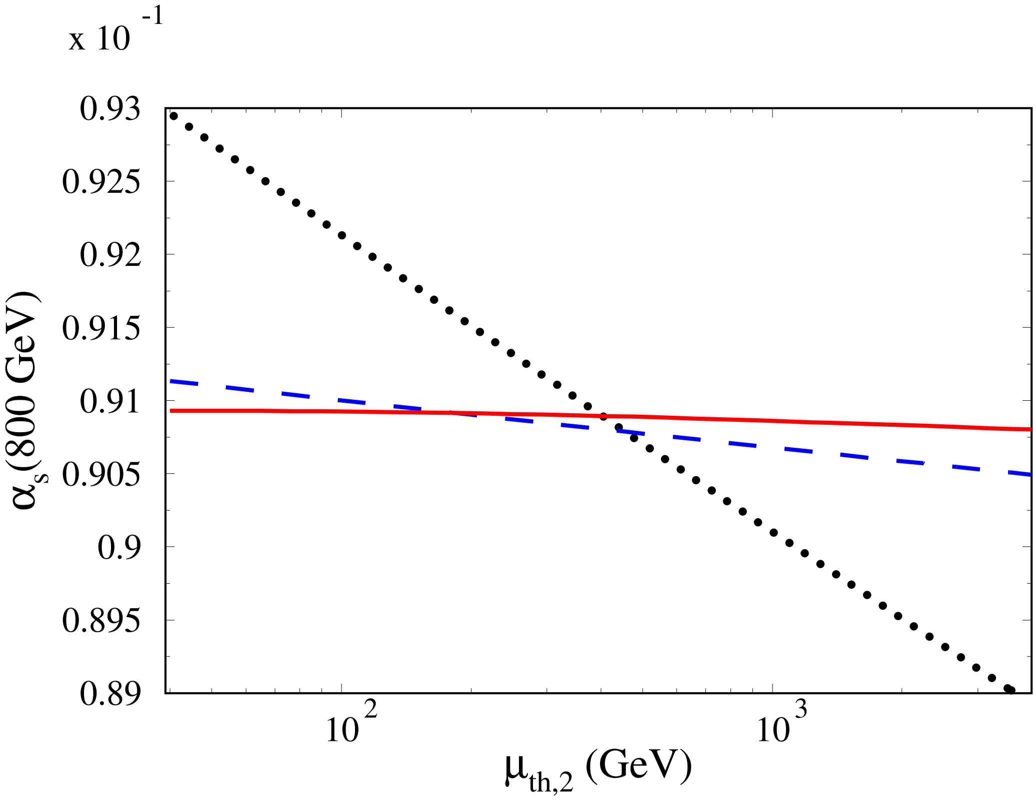

Figure 6: $\alpha_s(800\ \mathrm{GeV})$ as a function of $\mu_{\rm th,1}$ for scenario (C). The dotted, dashed and full lines correspond to one-, two- and three-loop running.

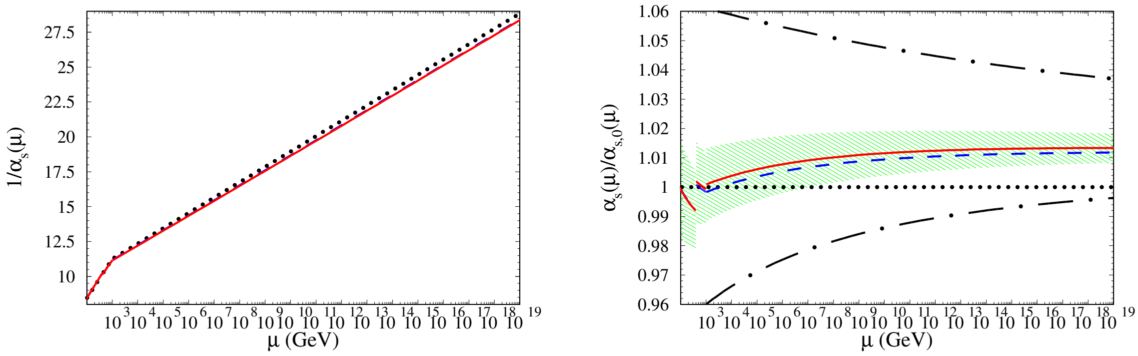

(a) (b)

Figure 7: (a) $\alpha_s(\mu)$ as a function of μ for scenario (C). The dotted, dashed and full lines correspond to one-, two- and three-loop running. (b) Ratio of $\alpha_s(\mu)$ and the corresponding leading order value corresponding to $\alpha_s^{\overline{\rm MS}}(M_Z) = 0.1187$ for scenario (C). The dotted and dashed lines correspond to one- and two-loop results, respectively. The (green) band corresponds to the uncertainty of α_s as given in Eq. (32). The dash-dotted lines corresponds to the three-loop result for scenario (D) where the SUSY masses are set to 400 GeV (upper line) and 2 TeV (lower line).

supersymmetric mass spectrum of the SPS1a reference point. The inner bands account for the expected improvements in the absolute errors due to the future experimental analysis at LHC+LC.

7 Conclusions

In order to get insight into the mechanism behind Grand Unification, it is necessary to have precise relations among the various couplings evaluated at the electro-weak and the GUT scale within the expected theoretical framework, in our case the MSSM. In this paper we provided the two-loop decoupling coefficients which, in combination with the known three-loop renormalization group equation, establish the three-loop relation between the strong coupling at M_Z and $\mu_{\rm GUT}$. Furthermore, they ensure the independence of the decoupling procedure from the scale at which the heavy particles are integrated out, up to higher order terms in α_s.

A large variation of $\alpha_s(\mu_{\rm GUT})$ results from the uncertainty in $\alpha_s(M_Z)$. However, as can be seen from Eq. (33) and Fig. 7(b), there is also a significant uncertainty from the values of the individual mass parameters. The effect of including the two-loop decoupling relation is a significant stabilisation of the dependence of $\alpha_s(\mu_{\rm GUT})$ on the matching scales.

The analysis of this paper is based on certain approximations concerning the mass pattern (cf. Eq. (6)) within the MSSM spectrum. This results in compact formulae. It is

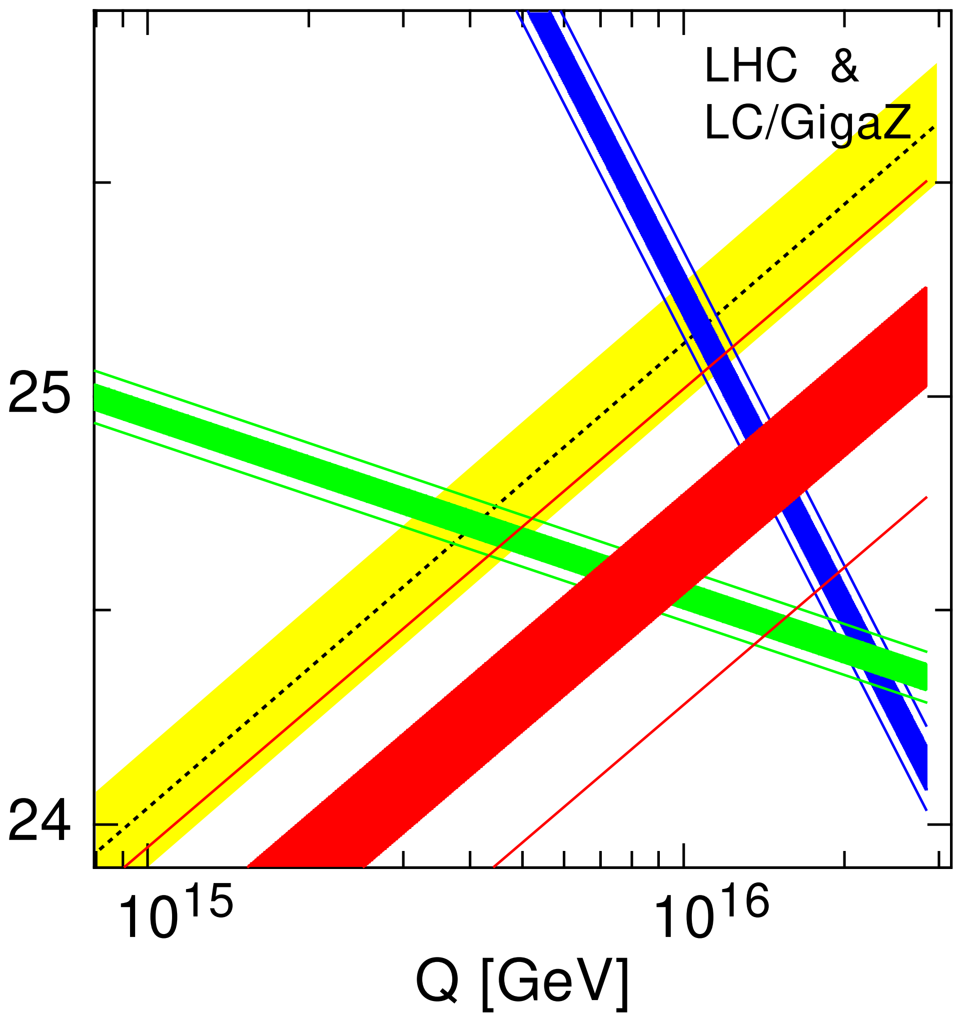

Figure 8: Running of the inverse couplings $1/\alpha_i$, $i = 1$ (blue band), 2 (green band), and s (red band) with two-loop accuracy around the unification point defined as the meeting point of α_1 and α_2. The wide error bands take into account present data and the supersymmetric mass spectrum from LHC measurements within mSUGRA. The narrow bands envisage the improvements expected from the LHC+LC coherent analysis [7]. The yellow band shows our results for $1/\alpha_s$ with three-loop accuracy.

desireable to derive in a future calculation more general formulae and investigate further the dependence on the quark masses.

Acknowledgements
This work was supported by the Sonderforschungsbereich Transregio 9. R.H. is supported

by *Deutsche Forschungsgemeinschaft* (contract HA 2990/2-1, Emmy-Noether program). We thank S. Heinemeyer and W. Porod for discussions and useful comments.

References

[1] S. Dimopoulos, S. Raby and F. Wilczek, Phys. Rev. D **24** (1981) 1681.

[2] L. E. Ibanez and G. G. Ross, Phys. Lett. B **105**, 439 (1981).

[3] U. Amaldi, W. de Boer and H. Fürstenau, Phys. Lett. B **260** (1991) 447.

[4] P. Langacker and M. Luo, Phys. Rev. D **44** (1991) 817.

[5] J. R. Ellis, S. Kelley and D. V. Nanopoulos, Phys. Lett. B **260** (1991) 131.

[6] G. A. Blair, W. Porod and P. M. Zerwas, Eur. Phys. J. C **27** (2003) 263 [arXiv:hep-ph/0210058].

[7] B. C. Allanach, G. A. Blair, S. Kraml, H. U. Martyn, G. Polesello, W. Porod and P. M. Zerwas, arXiv:hep-ph/0403133.

[8] See, e.g., `http://www-flc.desy.de/spa/`.

[9] T. Appelquist and J. Carazzone, Phys. Rev. D **11** (1975) 2856.

[10] W. Bernreuther and W. Wetzel, Nucl. Phys. B **197** (1982) 228 [Erratum-ibid. B **513** (1998) 758].

[11] K. G. Chetyrkin, B. A. Kniehl and M. Steinhauser, Nucl. Phys. B **510** (1998) 61 [arXiv:hep-ph/9708255].

[12] L. J. Hall, Nucl. Phys. B **178** (1981) 75.

[13] R. V. Harlander and M. Steinhauser, JHEP **0409** (2004) 066 [arXiv:hep-ph/0409010].

[14] N. Arkani-Hamed and S. Dimopoulos, [arXiv:hep-th/0405159].

[15] G. F. Giudice and A. Romanino, Nucl. Phys. B **699** (2004) 65 [Erratum-ibid. B **706** (2005) 65] [arXiv:hep-ph/0406088].

[16] K. G. Chetyrkin, B. A. Kniehl and M. Steinhauser, Phys. Rev. Lett. **79** (1997) 2184 [arXiv:hep-ph/9706430].

[17] M. Steinhauser, Phys. Rept. **364** (2002) 247 [arXiv:hep-ph/0201075].

[18] S. Heinemeyer, W. Hollik, H. Rzehak and G. Weiglein, Eur. Phys. J. C **39** (2005) 465 [arXiv:hep-ph/0411114].

[19] W. Siegel, Phys. Lett. B **84** (1979) 193.

[20] Z. Bern, A. De Freitas, L. J. Dixon and H. L. Wong, Phys. Rev. D **66** (2002) 085002 [arXiv:hep-ph/0202271].

[21] S. Eidelman et al., Phys. Lett. B **592** (2004) 1.

[22] D. M. Capper, D. R. T. Jones and P. van Nieuwenhuizen, Nucl. Phys. B **167** (1980) 479.

[23] T. Muta *Foundations of Quantum Chromodynamics*, World Scientific, Singapore, 1987.

[24] I. Jack, D. R. T. Jones and C. G. North, Phys. Lett. B **386** (1996) 138 [arXiv:hep-ph/9606323].

[25] D. M. Pierce, J. A. Bagger, K. T. Matchev and R. j. Zhang, Nucl. Phys. B **491** (1997) 3 [arXiv:hep-ph/9606211].

[26] A. I. Davydychev and J. B. Tausk, Nucl. Phys. B **397** (1993) 123.

[27] P. Nogueira, J. Comput. Phys. **105** (1993) 279.

[28] T. Seidensticker, [arXiv:hep-ph/9905298].

[29] R. Harlander, T. Seidensticker and M. Steinhauser, Phys. Lett. B **426** (1998) 125 [hep-ph/9712228].

[30] M. Steinhauser, Comput. Phys. Commun. **134** (2001) 335 [arXiv:hep-ph/0009029].

[31] S. A. Larin, T. van Ritbergen and J. A. M. Vermaseren, Nucl. Phys. B **438** (1995) 278 [arXiv:hep-ph/9411260].